

Field-induced modifications of hydrogenated diamond-like carbon films using a scanning probe microscope

V.D. Frolov*, V.I. Konov, S.M. Pimenov, E.V. Zavedeev

Natural Sciences Center of General Physics Institute, Vavilov str. 38, Moscow 119991, Russia

Available online 1 October 2004

Abstract

Low-conducting hydrogenated diamond-like carbon (a-C:H) films were examined for the purpose of nanometer-scaled modifications under the action of local electrical field. To create the modifications, a series of voltage pulses (either positive or negative, or bipolar) was applied between the sample and the cantilever at regular points along a given line while scanning the probe in contact mode under ambient conditions. It was established that both geometrical and electrical properties of the obtained nano-objects strongly depended on the pulse shape. A nanocavity with a well-conducting bottom was reproducibly formed under the bipolar voltage pulses. Otherwise, the actions mostly resulted in the formation of poorly conducting nanoprotusions. Evidence was obtained that, in the case of monopolar voltage pulse actions, local heating of the surface layer underneath the probe is a dominant process in the mechanism of the nanoprotusion formation. We consider that the bipolar pulse actions additionally involve the tip-surface electrostatic interaction which plays an important role in the formation of nanocavities.

© 2004 Elsevier B.V. All rights reserved.

Keywords: DLC films; Nanolithography; Nanostructures; Geometrical and electrical properties characterization

1. Introduction

Recent years, a number of materials were examined for the purpose of field-induced modifications using an air-operated scanning probe microscope (SPM). The formation of surface nanoprotusions was demonstrated in the experiments with silicon [1–4] and certain metals [5–8], which was considered to result from local oxidation at positive voltages, i.e., anodization of the sample surface underneath the probe in the presence of adsorbed water vapors.

A more complex behavior of the tip-induced surface modifications was observed for carbon materials such as amorphous carbon films, highly oriented pyrolytic graphite (HOPG) and diamond. For amorphous carbon films [9–12], either nanoprotusions or nanocavities were formed inside exposed areas, mostly depending on the positive voltage magnitude and ambient (air or vacuum) conditions.

For HOPG samples, a single pattern (i.e., only nanocavities) was registered under similar voltage regimes used [13]. In case of hydrogenated diamond surfaces, both types of the nanostructures were observed, the formation (and registration) of which was found to depend not only on the value of the applied bias voltage but also on the mode (contact or noncontact) of registration of the patterns produced [14,15].

Evidences were given that, above a threshold, the SPM actions led to local oxidation, whereby the uppermost surface layers were removed from the carbon films tested, i.e., nanocavities appeared [9,12,13]. To explain the patterning of the nanoprotusions in diamond-like carbon (DLC) films, phase transitions in carbon due to local heating of the material were proposed [10,12]. Another explanation, related to hydrogenated diamond surfaces, was done in Refs. [14,15], which described nanoprotusions as artifacts of SPM mapping, suggesting the accumulations of water adsorbate on oxidized areas to be responsible for the observed changes in topography images. So, a variety of

* Corresponding author. Tel.: +7 095 1326498; fax: +7 095 2323862.
E-mail address: frolov@ran.gpi.ru (V.D. Frolov).

reactions of carbon materials under the electrical field actions is of great interest and importance in the nanoscale surface modifications in ambient air.

In the present work, we focus on the field-induced modifications of a-C:H films (sheet resistance $R \sim 10^6 \Omega/\square$). Both geometrical and electrical properties of the obtained nanostructures are investigated by means of the SPM technique.

2. Experimental details

a-C:H films of 1 μm thick were grown on Si substrates by means of r.f. plasma chemical vapor deposition in C_2H_2 atmosphere. Details of the films growth were described elsewhere [16]. According to Ref. [16], deposition conditions were as follows: discharge power 750 W (about 250 mW/cm^2 of the substrate); pressure 2×10^{-2} Pa; growth rate 1 $\mu\text{m}/\text{h}$; substrate potential (1.76 MHz) $U=1$ kV. The sp^3/sp^2 ratio in the DLC films was determined from AES spectra: the content of sp^3 bonding was about 60% in the films grown at $U=1$ kV [16]. The film density is 2.4 g/cm^3 , and the sheet resistance is $10^6 \Omega/\square$. Some other properties (e.g., stability and chemical resistance of the films, mechanical properties) are also described in Ref. [16].

Experiments on the DLC film patterning were carried out in the air-operated SPM Solver P47 (NT-MDT, Russia), using cantilevers coated with conducting layers (TiN, TiO, Pt) as the probes for SPM actions, and also for testing the samples before and after the actions. As a preliminary step, a certain area was scanned in tapping mode in order to register the original surface relief. To create patterns, the probe was scanned along a given line in contact mode, and, during the scanning, a series ($N=1-5000$) of rectangular voltage pulses, either positive (regime 1) or negative (regime 2), or bipolar (regime 3), with the magnitude U in the range from -10 to $+10$ V and duration $\tau=0.1-1000$ ms was consecutively applied between the sample and the grounded probe at regular points distanced at $\Delta=6-60$ nm one from another. For bipolar actions, the pulse duration τ was defined as $\tau=\tau_++\tau_-$, where τ_+ , τ_- are the time intervals for the positive (U_+) and negative (U_-) voltage pulses, respectively ($\tau_+=\tau_-$ was chosen). Immediately after the actions, the mapping was repeated over the same scan area to reveal the relief deviations δH inside the exposed region. Finally, spreading resistance imaging (SRI) via current–voltage ($I-V$) characterizations in numerous (up to 64×64) points of the scan area was realized.

3. Experimental results and discussion

Mapping of the untreated a-C:H films reveals the surface relief with ~ 0.15 nm roughness which limits the control of δH after patterning. In general, the results of our experiments can be described as follows.

3.1. Surface relief deviations under monopolar voltage pulses

When the magnitude $|U|$ exceeds the value of ~ 5 V, both the positive and negative pulse actions become to influence the exposed area that mostly leads to the formation of ridge-like nanoprotusions ($\delta H > 0$), as shown in Fig. 1. Near the threshold, the ridge width is $L \sim 50$ nm, and it is widened to $L=150-200$ nm when $|U| \geq 7$ V. If the parameters N , τ , Δ are kept constant, the protrusion height is monotonically rising with increasing bias voltage. At $|U|=\text{const.}$, the peak height H is proportional to the total ‘exposure time’ of a given point, i.e., $H \propto N\tau(L/\Delta)$. Hereinafter, we consider that each series of SPM actions results in the modification of a sample area of diameter $d \approx L$. Because of this, the modification at a given point is repeated about L/Δ times. Hence, the term $N\tau L/\Delta$ characterizes the dwell time of actions (T_d) with respect to the fixed point. In logarithmic coordinates, the $H(T_d)$ data is approximated by the line with slope $n \approx 1$ that indicates the linear dependence $H=S_p T_d$, where S_p is the modification rate per a single pulse for nanoprotusions. It should be particularly noted that no saturation is observed for H in our experiments. At $|U|=10$ V, the rate S_p for the positive voltage pulses reaches the maximum value $S_p=0.65$ nm/s that is at least two times higher than that for the negative voltage pulses. For example, at $|U|=10$ V, $N=500$, $\tau=1$ ms, $\Delta=20$ nm, regime 1 ($U>0$) produces the patterns of $H=1.5-4.0$ nm height, whereas regime 2 ($U<0$) leads to $H=0.5-1.0$ nm.

Some features of the modification process should be particularly noted. As is seen from the surface profile in Fig. 1c and also from Fig. 2a, the produced nanostructures are not uniform in height. In addition, the DLC material modified as a result of the SPM actions is found to be mechanically ‘softer’ than the original film. This effect is illustrated in Fig. 2b obtained after scanning the area (shown in Fig. 2a) in contact mode (at $U=0$). As is seen from Fig. 2, the protrusion (bright stripe in Fig. 2a) is partly transformed to the cavity (dark stripe in Fig. 2b). Since the contact mode is used in the SPM processing, scratching the surface most likely leads to peeling of the mechanically unstable material from the substrate.

3.2. Surface relief deviations under bipolar voltage pulses

On the contrary to the previous case, nanocavities in the form of grooves can be directly patterned using the bipolar voltage pulse actions. As an example, Fig. 3 demonstrates the inscription ‘GPI’ (abbreviation of ‘General Physics Institute’) on the DLC film surface; the patterns of depth $D \sim 30$ nm and width $L \sim 150$ nm were formed under the bipolar voltage pulse regime. The groove appears only if the positive bias exceeds the value $U_+ \sim 5$ V that is practically coincident with the threshold for patterning of

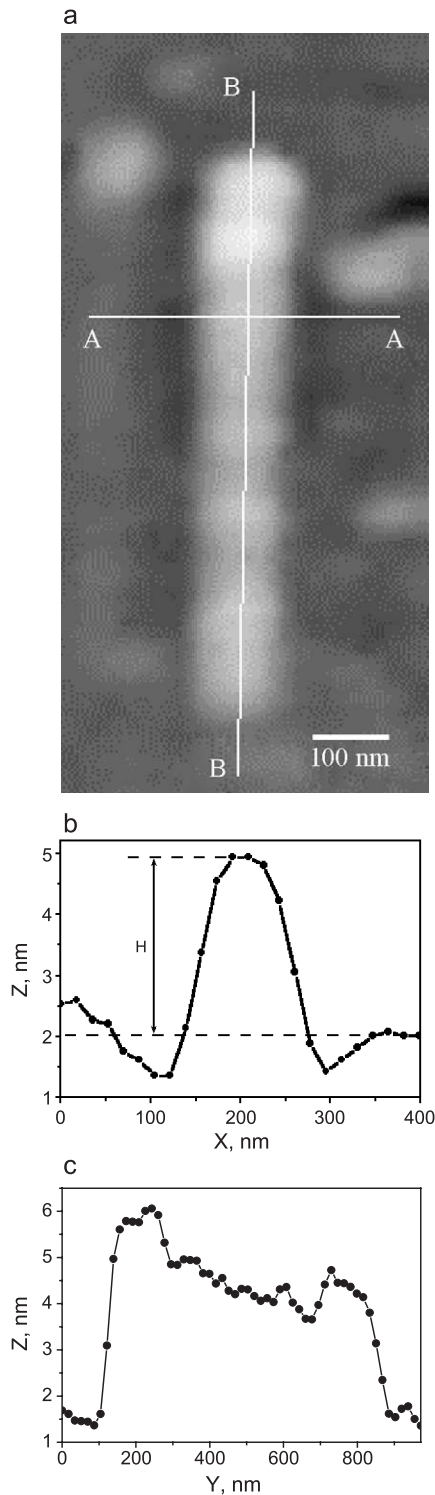


Fig. 1. The field-induced nanoprotusion on the a-C:H film surface (regime 1, $U=10$ V, $N=500$, $\tau=1$ ms, $\Delta=20$ nm): (a) topography; (b) surface profile made along the line AA; (c) surface profile made along the line BB.

the nanoprotusions under the monopolar voltage pulse actions. The sufficiency condition is that the negative bias U_- must exceed a definite value, depending on the positive bias magnitude. In particular, this value is $U_- \sim 2.5$ V at $U_+=10$ V that is illustrated in Fig. 4, where the

δH_m vs. U_- plot is presented (in the plot, $\delta H_m > 0$ for nanoprotusions, and $\delta H_m < 0$ for nanocavities). When the positive bias decreases to $U_+ \sim 5$ V, the corresponding threshold for U_- increases to $U_- \sim 5$ V. A correlation between the dwell time T_d and the groove depth D is found quite different from a linear dependence. So, the $D(T_d)$ data obtained at $U_+=U_-=\text{const.}$ (symmetrically biased pulses) can be fitted by the formula $D \propto T_d^{1/3}$. It means that the modification rate per a single pulse $S_c = D/T_d$, which defines the efficiency of the nanocavity formation, tends to zero at extremely long exposures. From the standpoint of formal logic, such behavior can be considered as a result of two competing processes, namely ‘graphitization’ (swelling, see discussion below) and material removal, which occur at the same rate during long exposures. However, a simplest explanation is that the conditions for cavity formation, e.g., due to an increase of the tip-surface contact area during penetrating the tip into the film, permanently deteriorate. Nevertheless, being inspected over available exposures, the rate S_c stays at a higher level as compared to the rate S_p for nanoprotusions (for example, $S_c \sim 1.5$ nm/s at $U_+=U_-=10$ V, $N=1000$, $\tau=2$ ms, $\Delta=20$ nm).

3.3. Electrical properties of patterns

The SRI of patterns shows super-linear, symmetrical $I-V$ characteristics for both the untreated and exposed film areas. Fig. 5 displays the comparative profiles of the film surface relief and electroconductivity (electron current at the applied voltage $U_b=5$ V), registered after two consecutively realized SPM actions: (i) positive pulse actions at the position $X=250$ nm, and (ii) bipolar pulse actions at $X=650$ nm. The resulting patterns are the nanoprotusion of ~ 5 nm height and ~ 100 nm width, and the nanocavity of ~ 12 nm depth and ~ 200 nm width, respectively. As is seen from Fig. 5, the nanoprotusion conductivity is close to that of the untreated film area whereas the nanocavity bottom exhibits much higher (two orders of magnitude higher) conductivity than the original film. Note that only the bottom region (at $X \approx 680$ nm) of the cavity exhibits the high conductivity while an ‘adjacent valley’ (at $X \approx 580$ nm) shows the low conductivity value. The nonuniform depth profile (i.e., ‘two-valley’-like profile) of the cavities is also observed in the patterns in Fig. 3 that probably might be due to the shape of the tip used and, therefore, to the specific properties of the contact between the tip and the surface.

Here we shortly discuss about the field-induced processes and possible physical mechanisms responsible for the formation of nanostructures in the DLC films and, especially, the pulse shape effect observed. In early [9] and recent [12] papers on SPM nano-processing of hard DLC films, it is established that two bias-dependent processes—phase transition (‘graphitization’) and oxidation, govern the formation of nanoscale surface features

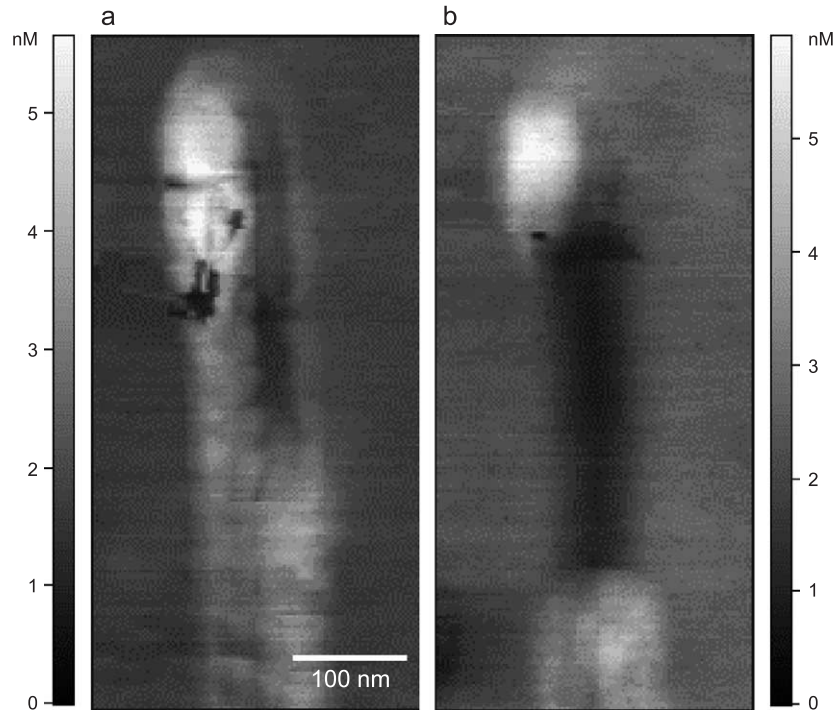


Fig. 2. Pattern on the a-C:H film surface: (a) the initial image, (b) the image after scanning the area in contact mode (at $U=0$).

(either protrusions or grooves) caused by local deposition of thermal energy at the ‘tip-film surface’ contact. Generally, local surface heating of hard a-C:H films results in hydrogen effusion and ‘amorphous-to-graphite-like’ structure transformation, which is accompanied by a decrease of the film density (pronounced as the surface swelling) [17,18]. These processes begin to occur at 300–350 °C [17,19] followed by oxidation of the ‘graphitized’ surface layer at higher temperatures (of about 600 °C [12,17]).

Our data on the nanoprotrusion formation under the actions of both the positive and negative voltage pulses also support the thermal mechanism and, particularly, the initial ‘graphitization’ stage which should be pronounced at lower temperatures (in the region of the tip-surface contact) than

the oxidation process. The fact that the transition to the tip-induced oxidation was not observed over the applied voltage range ($-10 \text{ V} \leq U \leq +10 \text{ V}$) can indicate that the local surface temperature required for intensive oxidation to occur was not achieved, e.g., because of specific properties of the tip-to-film contact.

It is however surprisingly that applying the bipolar voltage pulses resulted in remarkable changes in the produced nanostructures, i.e., the threshold effect of the nanocavity formation. It would be more logical to expect that the action of two successive voltage pulses of equal magnitude and different polarity (e.g., $U_1=+10 \text{ V}$ and $U_2=-10 \text{ V}$) should lead to an increase in the nanoprotrusion height, as it follows from the data on the monopolar pulse regimes. Formally, this means that the tip-induced oxidation

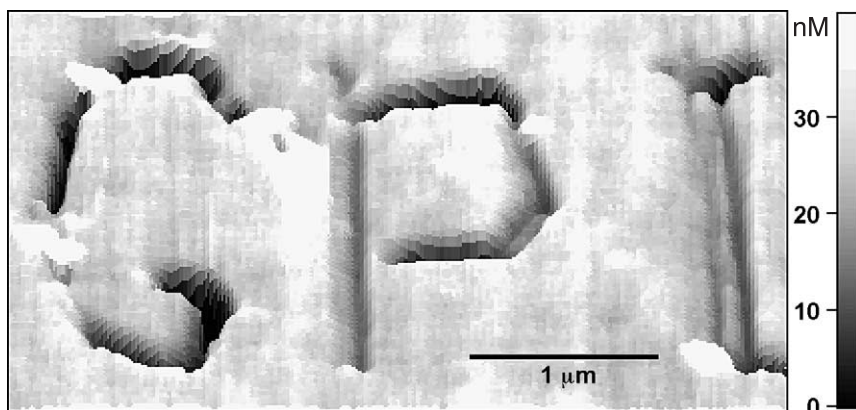


Fig. 3. AFM image of the inscription ‘GPI’ patterned on the a-C:H film surface in regime 3 ($U_+=U_-=10 \text{ V}$, $N=1000$, $\tau=1 \text{ ms}$, $\Delta=20 \text{ nm}$).

is not the only mechanism in the observed nanocavity formation, and that other nonthermal mechanisms can be also important. In other words, there should be an additional factor ('driving force') which would promote the tip-induced oxidation under the particular patterning conditions with bipolar pulses.

We suggest to consider a role of charging phenomena (charging of deep traps in DLC films [20]) and its influence on electrostatic interaction between the tip and the DLC film in the course of the bipolar pulse actions. Experimental data of recent publications [21,22] evidence that, indeed, charge-transfer processes can play an important role in SPM characterization of the DLC films with a biased tip. So, we suppose that during the positive bias action the electron current through the modified surface layer is accompanied by trapping the injected electrons within a low-conducting phase. As a result of charge trapping the DLC surface is negatively charged, and during the negative bias action the electrostatic attractive force between the tip and the charged material is strongly enhanced. If so, it is assumed that three interrelated processes could cause the material removal in the course of the nanocavity formation. First, the tip-to-charged surface attraction can generate high internal stresses in the surface layer. Would the stress exceed the tensile strength of the modified surface layer (which, as mentioned above, is mechanically softer than the original DLC), a spallation-like removal may be possible similar to the laser-induced spallation observed in the same a-C:H film [18]. Second, the attraction force increases the load of the tip onto the substrate that, in turn, can provide the removal of 'soft' material by mechanical scratching. Third, the enhanced electrostatic 'tip-to-surface' attraction changes the properties of the tip-surface contact which can lead to increasing temperature underneath the probe and, as a result, to initiating the oxidation process. Which of them has a major effect in the mechanism of the nanocavity formation requires further investigations (first of all, SPM nanostructuring of DLC films in vacuum or inert atmosphere), but, in any case, the charging processes seem to be very

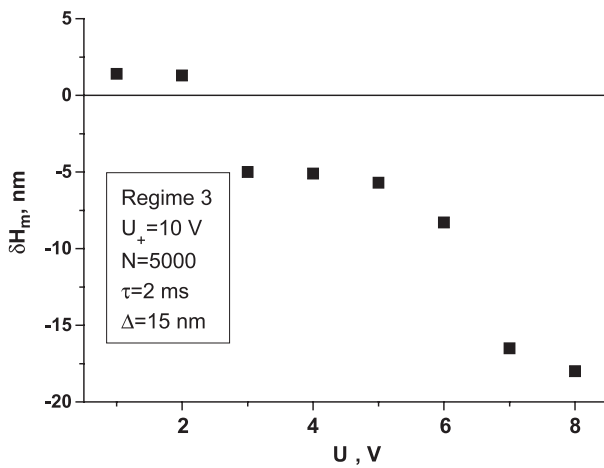


Fig. 4. The ΔH_m vs. U_- plot at $U_+ = \text{const}$.

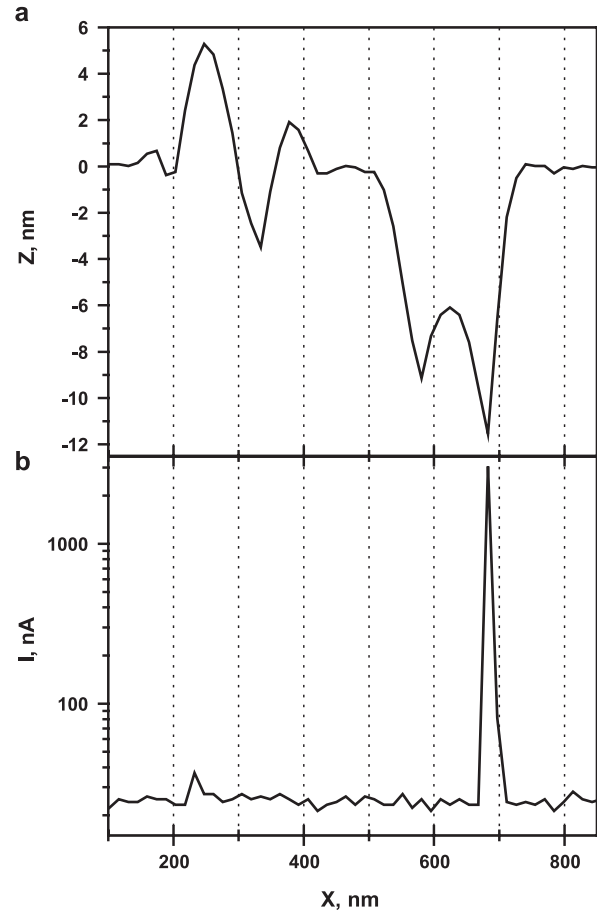


Fig. 5. Comparative profiles of (a) the film surface relief, and (b) electroconductivity after two consecutively realized SPM actions: with positive pulses at the position $X=250$ nm, and with bipolar pulses at $X=650$ nm.

important and should be taken into account under the bipolar pulse regime.

4. Conclusions

Field-induced modifications of the a-C:H films under the actions of voltage pulses have been studied by means of SPM technique. It was established that both geometrical and electrical properties of the obtained nano-objects strongly depended on the pulse shape. Evidence was obtained that, in the case of monopolar voltage pulse actions, local heating of the surface layer underneath the probe is a dominant process in the mechanism of the nanoprotusion formation. We consider that the bipolar pulse actions additionally involve the tip-surface electrostatic interaction which plays an important role in the formation of nanocavities.

From the standpoint of practical applications, an important result is that the bipolar voltage pulse actions provide the patterns with increased conductivity. It gives a possibility to form conducting channels in the a-C:H films that can be used in engineering of nanoelectronic elements, in particular, nanoemitters of electrons.

Acknowledgements

The work was partly supported by the Russian Foundation for Basic Research, under Grant No. 02-02-16725.

References

- [1] J.A. Dagata, J. Schneir, H.H. Harary, C.J. Evans, M.T. Postek, J. Bennett, *Appl. Phys. Lett.* 56 (1990) 2001.
- [2] H.C. Day, D.R. Allee, *Appl. Phys. Lett.* 62 (1993) 2691.
- [3] E.S. Snow, P.M. Campbell, *Appl. Phys. Lett.* 64 (1994) 1932.
- [4] P. Avouris, T. Hertel, R. Martel, *Appl. Phys. Lett.* 71 (1997) 285.
- [5] H. Sugimura, T. Uchida, N. Kitamura, H. Masuhara, *Appl. Phys. Lett.* 63 (1993) 1288.
- [6] S. Gwo, C.-L. Yeh, P.-F. Chen, Y.-C. Chou, T.T. Chen, T.-S. Chao, S.-F. Hu, T.-Y. Huang, *Appl. Phys. Lett.* 74 (1999) 1090.
- [7] E.S. Snow, D. Park, P.M. Campbell, *Appl. Phys. Lett.* 69 (1996) 269.
- [8] D. Wang, L. Tsau, K.L. Wang, P. Chow, *Appl. Phys. Lett.* 67 (1995) 1295.
- [9] T. Mühl, H. Brückl, G. Weise, G. Reiss, *J. Appl. Phys.* 82 (1997) 5255.
- [10] T.W. Mercer, N.J. DiNardo, J.B. Rothman, M.P. Siegal, T.A. Friedmann, L.J. Martinez-Miranda, *Appl. Phys. Lett.* 72 (1998) 2244.
- [11] S.C. Eagle, G.K. Fedder, *Appl. Phys. Lett.* 74 (1999) 3902.
- [12] S. Myhra, *Appl. Phys., A* (2003) doi:10.1007/S00339-003-2370-7, published online: 4 December 2003.
- [13] T.R. Albrecht, M.M. Dovek, M.D. Kirk, C.A. Lang, C.F. Quate, D.P.E. Smith, *Appl. Phys. Lett.* 55 (1989) 1727.
- [14] M. Tachiki, T. Fukuda, K. Sugata, H. Seo, H. Umezawa, H. Kawarada, *Jpn. J. Appl. Phys.* 39 (2000) 4631.
- [15] B. Rezek, C. Sauerer, J.A. Garrido, C.E. Nebel, M. Stutzmann, E. Snidero, P. Bergonzo, *Appl. Phys. Lett.* 82 (2003) 3336.
- [16] V.F. Dorfman, B.N. Pypkin, *Surf. Coat. Technol.* 48 (1991) 193.
- [17] V. Yu. Armejev, E.N. Loubnin, V.G. Ralchenko, V.E. Strelitskiy, *Appl. Phys. Lett.* 58 (1991) 2758.
- [18] T.V. Kononenko, S.M. Pimenov, V.V. Kononenko, E.V. Zavedeev, V.I. Konov, G. Dumitru, V. Romano, *Appl. Phys., A* 79 (2004) 543.
- [19] Z.L. Akkerman, H. Efstathiadis, F.W. Smith, *J. Appl. Phys.* 80 (1996) 3068.
- [20] B. Druz, I. Zaritskiy, J. Hoehn, V.I. Polyakov, A.I. Rukovishnikov, V. Novotny, *Diamond Relat. Mater.* 10 (2001) 931.
- [21] T. Inoue, D.F. Ogletree, M. Salmeron, *Appl. Phys. Lett.* 76 (2000) 2961.
- [22] R.J.A. van den Oetelaar, L. Xu, D.F. Ogletree, M. Salmeron, H. Tang, J. Gui, *J. Appl. Phys.* 89 (2001) 3993.